Research Article

Khalid Guma Biro Turk*, Abdulrahman O. Alghannam, Faisal Ibrahim Zeineldin

Monitoring of hourly carbon dioxide concentration under different land use types in arid ecosystem

https://doi.org/10.1515/biol-2022-0534
received August 30, 2022; accepted November 13, 2022

Abstract: Air pollution is a major factor affecting human life and living quality in arid and semiarid regions. This study was conducted in the Al-Ahsa district in the Eastern part of Saudi Arabia to measure carbon dioxide (CO_2) concentration over different land-use types. Initially, the study's land use/land cover (LULC) was classified using the spectral characteristics of Landsat-8 data. Then, sensors were placed in five sites of different LULC types to detect CO_2, air temperature, and relative humidity. The Friedman test was used to compare CO_2 concentration among the five sites. Five LULC types were identified over the study area: date palm, cropland, bare land, urban land, and water. The results indicated that CO_2 concentration showed a maximum mean value of 577 ppm recorded from a site dominated by urban lands. During the peak time of human transportation, a maximum value of 659 ppm was detected. The CO_2 concentration mean values detected for the other LULC types showed 535, 515, and 484 ppm for the bare land, cropland, and date palm, respectively. This study's sensors and procedures helped provide information over relatively small areas. However, modelling CO_2 fluctuations with time for LULC changes might improve management and sustainability.

Keywords: air pollution, carbon dioxide, land use/land cover

*** Corresponding author: Khalid Guma Biro Turk,** Water Studies Center, King Faisal University, Al-Ahsa, 31982, Saudi Arabia, e-mail: kturk@kfu.edu.sa, khalidturk76@yahoo.co.uk
Abdulrahman O. Alghannam: Department of Agriculture Systems Engineering, College of Agricultural and Food Sciences, King Faisal University, P.O. Box 420, Al-Hassa 31982, Saudi Arabia
Faisal Ibrahim Zeineldin: Water Studies Center, King Faisal University, Al-Ahsa, 31982, Saudi Arabia

1 Introduction

Air quality, air-condition, and climate are major factors affecting human life and living quality [1]. The atmospheric carbon dioxide (CO_2) resulting from photosynthesis plays a major role in vegetation growth and is a crucial greenhouse gas (GHG) that contributes to global warming [2]. The carbon balance of arid regions can be significantly affected by environmental stresses and human activities [3,4]. The trend of the world population is to inhabit cities by 2050 [5], which might reflect the importance of decreasing GHG emissions [6]. As a result, the global mean concentration of CO_2 rose steadily from approximately 280 ppm to a level exceeding 400 ppm in the present [7].

Land use/land cover (LULC) changes due to urban expansion are considered crucial factors affecting CO_2 emissions [8]. LULC change affects the climate through changes in CO_2 fluxes between the land and the atmosphere [9] and accounting for approximately 10–15% of the atmospheric increase in CO_2 concentrations [10,11]. However, the LULC change can modulate the land–atmosphere CO_2 flux at a regional scale compared to the effects of GHG [12]. The direct and indirect GHG emissions from land-use activities such as livestock farming, manure management, fertiliser use, and paddy rice contribute around 12% of today's total GHG emissions and about 10% rise in CO_2 emissions from deforestation [13,14]. Nevertheless, terrestrial ecosystems can play an important role in sequestering atmospheric CO_2 for mitigating the GHG effect [15,16].

The observation of the land surface temperature (LST) in Shenyang, China, indicated that it was higher in urban and bare lands compared to agricultural and green lands [17]. The impact of the local climate zones (LCZ) on LST was investigated in Shenyang city, China's urban and rural areas, by Zhao et al. [18]. Their findings showed that the LST of LCZs did not follow a fixed order, as they changed from one month to another depending on

the land-use type in the urban and rural areas. Therefore, monitoring CO_2 concentration in urban areas is essential to measure the CO_2 emission from cities and estimate its contribution to the regional carbon budget [19]. CO_2 fluxes in urban areas are affected by the vegetative cover, human activity, and climate factors such as precipitation and temperature [20,21]. However, it is crucial to separate the influences of climatic factors for air pollution and environment management controlling over different land-use systems [22]. In cities, the CO_2 fluxes are controlled by fuel combustion from vehicles, industries, and buildings rather than biological processes [23,24]. Vegetation cover in urban areas can significantly influence the daily and seasonal patterns of the CO_2 balances [25].

Climate change and LULC change significantly affect CO_2 dynamics, and the main drivers are temperature and precipitation [26]. For example, the regional drought due to climate change in the lower Mississippi River Valley affected vegetation productivity, net carbon exchange flux, and atmospheric CO_2 concentration. Thus, the productivity in the drought area decreases by 23% [27]. The intervention of climate change and LULC changes and their impacts on the CO_2 process were investigated at a global scale using various climate change models; accordingly, for further reading, interested readers are advised to use the following cited literature [11,28–33].

Monitoring CO_2 levels is an important research theme in most parts of the world [34]. Therefore, a wide range of CO_2 sensors was developed using different materials for monitoring CO_2 concentration. A semiconductor sensor was used for detecting CO_2 for environmental observations [35]. Also, CO_2 sensors made of solid electrolytes [36–39], optic fibres [39], laser diodes [7], and non-dispersive infrared (NDIR) [40,41] detectors were utilised for observing CO_2 emissions.

The atmospheric measurement of the CO_2 concentration depends widely on NDIR sensors because they are stable and robust against interference by other air components, including pollutants [19]. In addition, the NDIR has excellent durability, which makes it the most popular sensor for measuring atmospheric CO_2 [41]. The calibrated NDIR sensors can reasonably provide accurate air CO_2 concentrations [7].

In Saudi Arabia, the increasing population within the urban and sub-urban areas puts pressure on natural resources and increases the hazard of CO_2 emissions. The study area's land-use system, located in the Eastern part of Saudi Arabia, showed a significant increase in urban lands during the last three decades [42]. Estimating CO_2 emissions from the LULC changes is considered uncertain due to the difficulty of assessing this flux from measurements [43]. However, in this study, direct measurements of CO_2 were made to investigate its flux along with the different LULC systems. Hence, the emergence of different patterns of land-use systems in the region will inevitably affect the amounts of CO_2 emitted. Also, the land-use system usually effectively represents the spatial distribution of CO_2 emissions and carbon sinks [44]. These conditions necessitate the importance of CO_2 observation under different arid lands and zones. Therefore, the main objective of this study was to measure CO_2 concentration over different land-use types. Also, an attempt was made to analyse the impact of CO_2 emissions on the arid ecosystem of the study area.

2 Materials and methods

2.1 Study area

The study was carried out in five sites in the Al-Ahsa District located in the Eastern part of Saudi Arabia (Figure 1). The area has a population of 1.1 million (https://www.stats.gov.sa/) and is dominated by a hot, desert climate [45]. The seasonal average temperatures might reach 45°C in summer and 5°C in winter. The rainfall is present only in winter, with less than 250 mm per annum [46]. The land-use system in the study area is predominated by agricultural activities that include date palm plantation and cropping of rice and vegetables. The study sites have different land-use types, areas, and elevations, although they are located in the same climatic zone (Table 1).

2.2 LULC classification

The LULC classification of the study area was conducted using the Landsat-8 image (path/row is 164/042) acquired on 17 July 2014 (Figure 1) from the United States Geological Survey (https://earthexplorer.usgs.gov/). The Landsat-8 image obtained corresponds with the CO_2 and climate data collected during the summer season of 2014. The image characteristics are shown in Table 2.

In order to identify the LULC within the study area, a field survey was conducted using a Global Positioning System instrument to obtain accurate location point data for each LULC class included in the classification process. The total number of the reference ground control points (GCPs) collected during the field survey was 110. The supervised maximum likelihood classification (MLC)

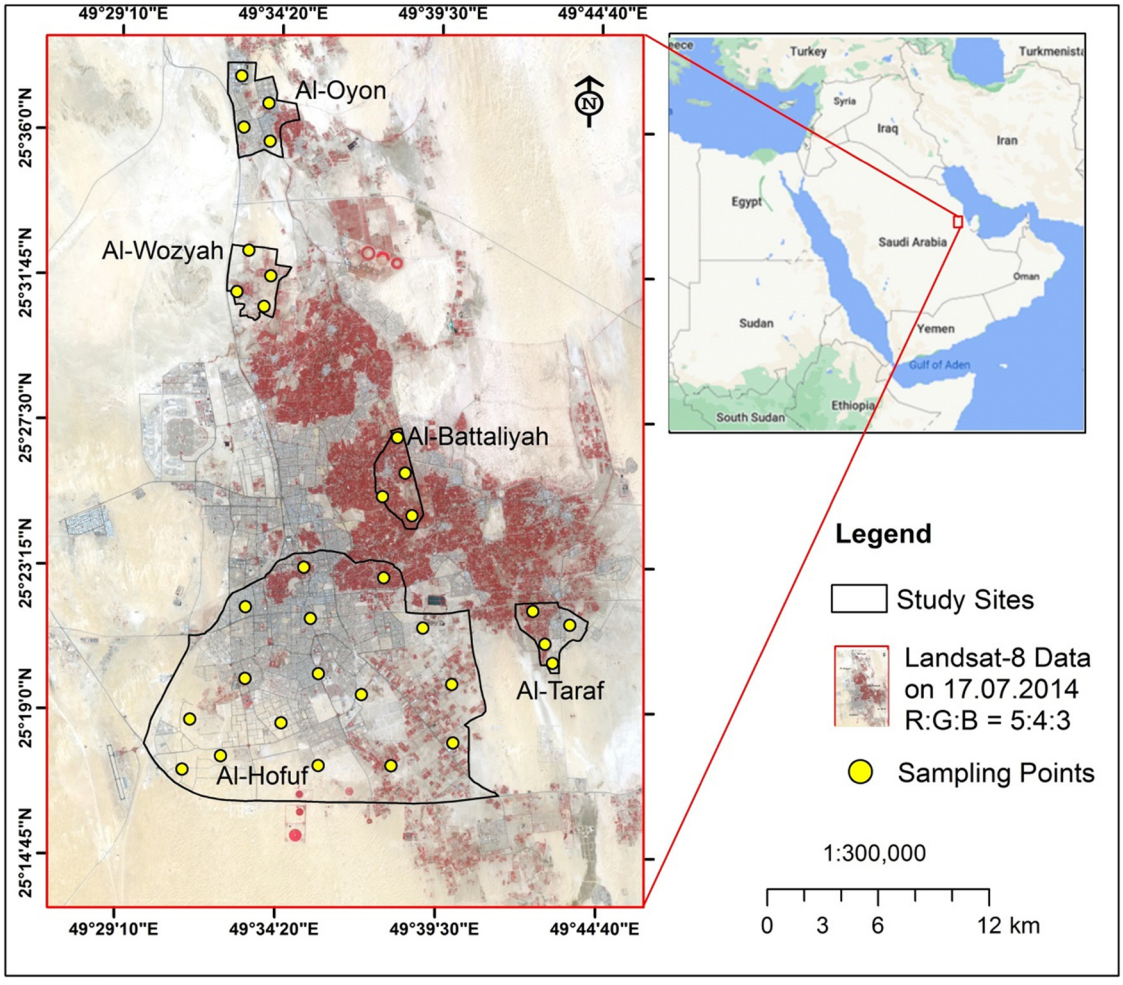

Figure 1: Location of the study sites within Al-Ahsa Zone. The background of the study sites is a Landsat-8 image acquired on 17 July 2014.

technique was applied to classify the image. MLC is valid and widely used in remote sensing for image classification [47–49]. For image accuracy assessment, 30% of the collected GCPs was used to validate the classification results. In addition, visual interpretation of the unclassified satellite image, Google Earth maps, and field observations were used to verify the LULC maps. The stratified random sampling method was adopted during the image classification to reduce bias [50]. The overall accuracy, user's and producer's accuracy, the Kappa statistic, and conditional Kappa were derived from the classification error matrices [51].

2.3 CO_2 and climate parameter measurements

The commercial GE Telaire 7001 carbon dioxide sensor measured CO_2 and temperature. The GE Telaire 7001 sensor was operating using the dual-beam NDIR technology, and it was connected to an analogue input on a HOBO H22 data logger. The sensor specifications are shown in Table 3, and it has independent CO_2 and temperature readings. The sensor has been factory calibrated and should be recalibrated once every 12 months using either a zero concentration gas or a gas with a specified concentration of CO_2 [52]. The sensors were distributed along with the study sites based on the area covered by each side. Accordingly, four sensors were fixed at each site in Al-Oyon, Al-Wozyah, Al-Battaliyah, and Al-Taraf, and a total number of 16 sensors were fixed in Al-Hofuf (Figure 1). The temperature (T) and relative humidity (RH) sensors were distributed following the same order as the CO_2 sensors. The sensors were distributed along the study site to assure data accuracy and fairness. In addition, the average sensor data from each site read the hourly CO_2, T and RH were collected to represent each site fairly. The wind speed data were collected during July 2014 from a local meteorological station in the study area.

Table 1: General characteristics of the five study sites and sampling time

Site	Latitude	Longitude	Area (km^2)	Elevation (m)	Start day and time	End day and time	Total hours (days)
Al-Oyon	25.61000	49.55700	13	112	01 July 2014 06:00:00 AM	30 July 2014 23:00:00 PM	714 (30)
Al-Wozyah	25.52900	49.55700	10	130	01 July 2014 06:00:00 AM	30 July 2014 23:00:00 PM	714 (30)
Al-Battaliyah	25.43000	49.63600	9	140	01 July 2014 06:00:00 AM	30 July 2014 23:00:00 PM	714 (30)
Al-Hofuf	25.32900	49.59800	192	155	01 July 2014 06:00:00 AM	30 July 2014 23:00:00 PM	714 (30)
Al-Taraf	25.35700	49.71700	8	125	01 July 2014 06:00:00 AM	30 July 2014 23:00:00 PM	714 (30)

2.4 Data analysis

The Friedman test was used to compare CO_2 concentration in the five sites. The Friedman test is a non-parametric analysis used to test the significance for more than two groups; it tests the null hypothesis [53]. Thus, Friedman's test determines whether the rank totals for each treatment differ significantly from the values expected by chance [54]. The computational formula for the Friedman test [54,55] is

$$X_r^2 = \frac{12}{nK(K+1)} \sum_{j=1}^{k} R_j^2 - 3nK(K+1), \tag{1}$$

where K is the number of groups (treatments), n is the number of subjects, and R_j is the sum of the ranked scores in each treatment. Numbers 12 and 3 are constants, not dependent on the number of subjects or experimental conditions. The test statistic X_r^2 is distributed according to the normal X_r^2 distribution with K–1 degrees of freedom when the rankings are random. As n and K increase, the approximation to the X_r^2 distribution improves.

Moreover, Kendall's W test was used to assess the agreement trend among the treatments. Kendall's W is referred to the normalization of the Friedman statistic, and it ranges from 0 to 1. The value "1" refers to the complete agreement between the raters, and "0" refers to the non-complete agreement between raters [56]. Therefore, Kendall's W can be calculated from Friedman's X_r^2 as follows [57]:

$$\hat{W}_{\text{kendall}} = \frac{X_r^2}{(K-1)}. \tag{2}$$

The Inverse Distance Weighted (IDW) tool of Geostatistical Analyst in the ArcGIS 10.2 software was used to perform data interpolation for the recorded CO_2 and produce the spatial distribution map [58].

The Statistica [59] and Microsoft Excel 2010 [60] software packages were used to perform the statistical analysis and produce graphs.

3 Results and discussion

3.1 LULC analysis

The study area analysis indicated that the existing LULC classes were the date palm, cropland, bare land, urban land, and water (Figure 2). However, within the study sites, the urban land occupied large areas in Al-Hofuf

Table 2: Characteristics of Landsat-8 data used in this study

Sensor	Bands type	Wavelength (μm)	Spatial resolution (m)
Operational Land Imager and Thermal Infrared Sensor	Band 1, Coastal aerosol	0.43–0.45	30
	Band 2, Blue	0.45–0.51	30
	Band 3, Green	0.53–0.59	30
	Band 4, Red	0.64–0.67	30
	Band 5, Near infrared	0.85–0.88	30
	Band 6, Short-wave infrared 1	1.57–1.65	30
	Band 6, Short-wave infrared 2	2.11–2.29	30
	Band 8, Panchromatic	0.50–0.68	15
	Band 9, Cirrus	1.36–1.38	30
	Band 10, Thermal infrared 1	10.60–11.19	100
	Band 10, Thermal infrared 2	11.50–12.51	100
Dataset attribute		**Attribute value**	
Land Cloud Cover		0.00	
Scene Cloud Cover L1		0.00	
Geometric RMSE Model		7.278	
Geometric RMSE Model X		4.239	
Geometric RMSE Model Y		5.916	

Table 3: Specifications of the GE Telaire 7001 CO_2 and temperature monitor

Standards	CO_2 channel	Temperature channel
Measurement range	0–10,000 ppm display	0–50°C display
Display resolution	±1 ppm	0.1°C
Accuracy	±50 ppm or ±5% for reading up to 5,000 ppm	±1°C
Response time	60 s for 90% of step change	20–30 min
Sample method	Diffusion or flow through (50–100 mL/min)	
Power requirement	100 mA peak, 20 mA average from 6 V	
Operating conditions	0–50°C, 0–95% RH, non-condensing	

compared to the other sites (Table 4). The date palm orchards were dominant in Al-Battaliyah concerning its relative total occupied area. Bare lands cover about 125 km^2 in Al-Hofuf, 7 km^2 for Al-Oyon and Al-Wozyah, and 1.4–3 km^2 in Al-Battaliyah and Al-Taraf (Table 4). The cropland areas ranged between 1 and 2 km^2 in all study sites and extended to 12 km^2 in Al-Hofuf. The LULC map of the study area showed how the different LULC classes were spatially distributed along with the study sites. Thus the LULC types were considered to affect the level of the CO_2 concentration in a varying way depending on the human activities at each site. Al-Hofuf represents one of the two largest city centres in the Al-Ahsa District. Therefore, urban lands extend in Al-Hofuf, covering large areas. In Saudi Arabia, many residents who lived in the major cities increased from 58% in 1975 to 82% in 2014 [61]. Most urban residents migrated to the cities to seek a modern lifestyle, better employment, and educational opportunities [62]. Also, the built-up area increased by 28.9% during 1990–2014 in Dammam, the capital of the Eastern Region in Saudi Arabia [48].

The overall accuracy of the classified LULC map was 90%, with a Kappa statistic of 86% (Table 4). However, the user's and producer's accuracies of different LULC classes ranged between 81 and 100%. Also, conditional Kappa coefficients for the different LULC types are shown in Table 5. The user's accuracy is the probability that a value predicted in a specific class is that class. That means it shows the reality on the ground. In statistical terms, the user's accuracy measures errors of commission. The producer's accuracy indicates the proportion of the reference data that are classified correctly for a given class. It corresponds to the statistical concept of errors of omission [49]. Urban lands show low conditional Kappa, user's and producer's accuracies compared to the other LULC

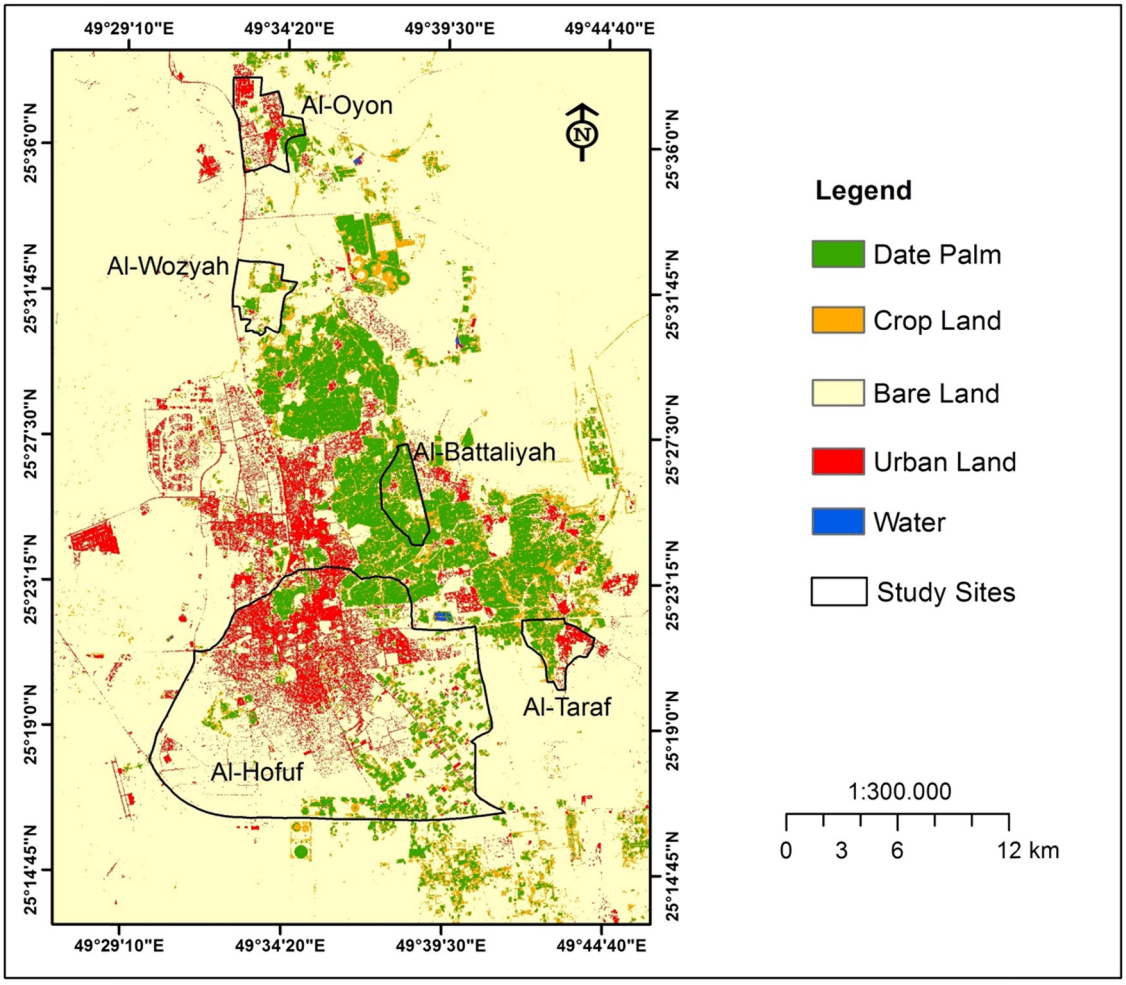

Figure 2: LULC map of the study area on 02 August 2014.

Table 4: Areas of LULC for the different study sites

LULC	Area (km^2)				
	Al-Oyon	**Al-Wozyah**	**Al-Battaliyah**	**Al-Hofuf**	**Al-Taraf**
Date palm	1.0	1.4	5.4	19.0	2.0
Cropland	1.0	1.2	2.0	12.0	1.0
Urban land	4.0	0.4	0.2	36.0	2.0
Bare land	7.0	7.0	1.4	125.0	3.0
Total area (km^2)	**13**	**10**	**9**	**192**	**8**

classes. This can be attributed to the misclassification of some urban land into bare land and cropland. On the other hand, bare lands and water recorded higher accuracies because they have less mixture than the other classes.

The hourly recorded *T* patterns are almost similar in all study sites showing a minimum value of 24°C and a maximum value of 52°C (Figure 3). However, the average *T* values ranged between 36 and 39°C; hence sites with large vegetation covers showed relatively low *T* compared to sites dominated by urban and bare lands. The variation of RH along the study sites is clearly shown in Figure 4. The minimum detected RH was 24%, while the maximum was 82%. However, the mean values ranged between 29 and 36%. The low amount of RH can be found during the early morning hours, while the high values occur during the day and most of the evening. Nevertheless, the highest

Table 5: Accuracy assessment of LULC classification

LULC	Classification accuracy (%)		
	User's	Producer's	Conditional Kappa
Date palm	92	91	89
Cropland	81	83	78
Bare land	94	93	89
Urban land	79	81	76
Water	100	100	100
Overall accuracy (%)	**90**		
Kappa statistic (%)	**86**		

RH value was observed in the site dominated by vegetation cover. The average daily wind speed over the study sites showed a minimum value of 3 km/day and a maximum value of 15 km/day (Figure 5). The dominant wind direction was north to north-west. High wind speed resulted in increasing T in urban lands, while the low wind speed decreased the RH in the sites with high vegetation cover.

In urban areas, the physical environmental parameters, including climatic factors, influence pollutant dispersion, which might increase heat island [63]. Therefore, considering the meteorological conditions is important when developing policies to control urban air quality [64].

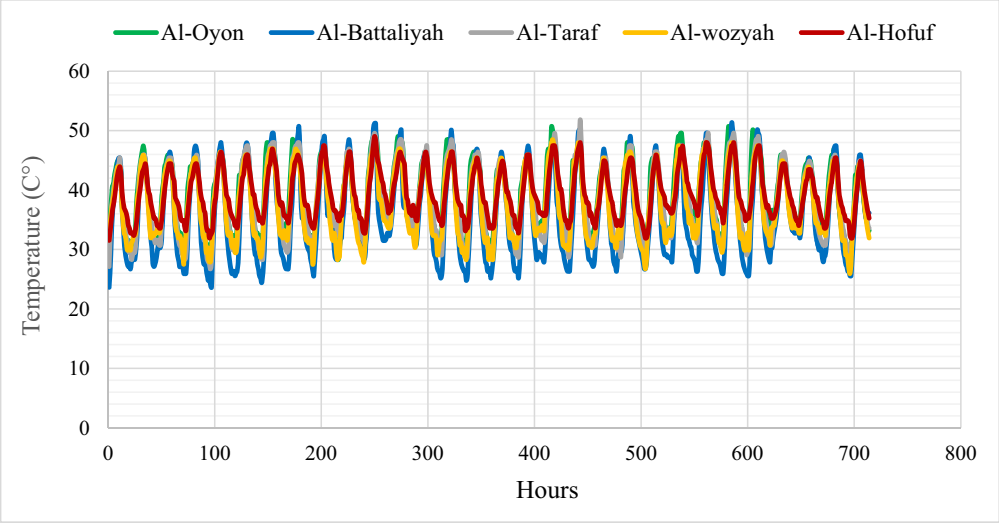

Figure 3: Hourly time series for the T levels in the different study sites during July 2014.

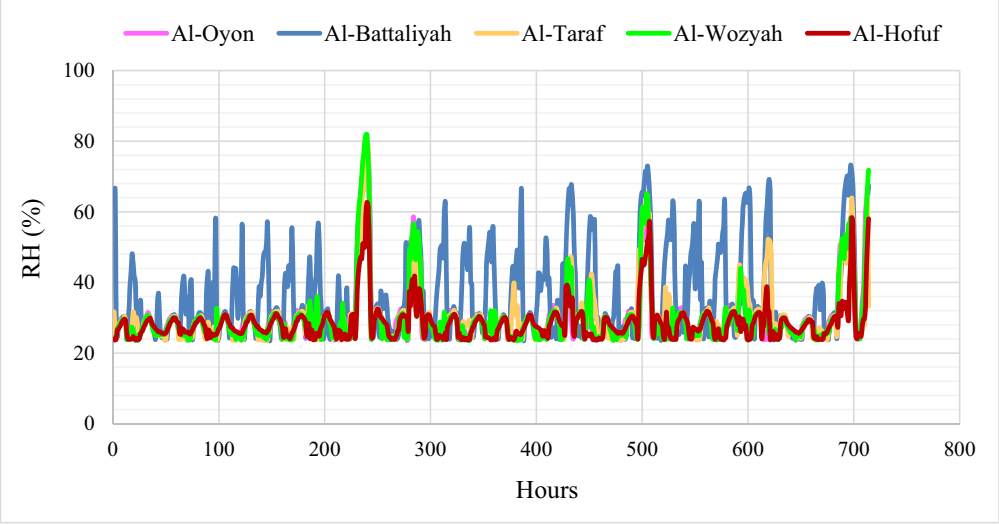

Figure 4: Hourly time series for the RH in the different study sites during July 2014.

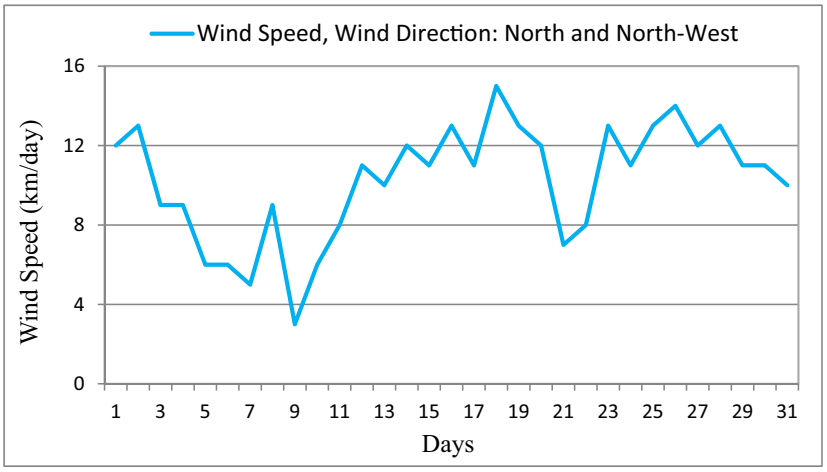

Figure 5: Average daily wind speed over the study area during July 2014.

3.2 CO_2 concentration and levels

The spatial distribution of CO_2 over the different study sites showed high concentration levels in Al-Hofuf and Al-Wozyah, followed by Al-Battaliyah and Al-Taraf. In contrast, low levels were detected in Al-Oyon (Figure 6). The CO_2 maximum mean value (μ^) of 577 ppm was observed in Al-Hofuf, while a minimum mean value of 391 ppm was detected in Al-Oyon (Figure 7). However, the statistical analysis of the CO_2 levels indicated significant differences ($P < 0.001$) among the study sites based on the Friedman test. Nevertheless, no significant difference ($P < 0.001$) was observed between Al-Battaliyah and Al-Taraf (Table 6). The low value of the $\hat{W}_{\text{kendall}}$ test (0.2) indicates that the levels of the CO_2 differed across the study sites (Figure 7). The hourly time series of the CO_2 levels were consistent with the spatial distribution of the CO_2 concentration for the different sites (Figure 8). The time series identified high values of 500–659 ppm and low 356–450 ppm for the CO_2 concentration among the study sites. In addition, the fluctuations of CO_2 concentration showed high levels during the peak time of transportation at 7:00–9:00 AM, 1:00–3:00 PM, and 7:00–9:00 PM.

The high concentration levels of the CO_2 in Al-Hofuf can be attributed to large urban land domination compared to the other sites (Figure 2). The fuel combustion from the cars in Al-Hofuf and the absence of public transport make the situation worse due to the increasing number of private vehicles. In the urban cities of Saudi Arabia, about 92% of the populations depend on private transportation. However, only 32% of these cities are accessible and linked to public transport systems [65]. Also, the energy use in Al-Hofuf is high compared to the suburban areas of the Al-Ahsa district due to the increase in the human population. Therefore, urban areas act as the primary source of CO_2 to the ambient air [66]. However, the ambient CO_2 levels could affect the air quality by involving isoprene emission in the vegetated areas [67,68]. Bare lands were the dominant land-use system in Al-Hofuf; therefore, during the summertime in July, this condition might increase the rate of CO_2 emissions due to the high-temperature degrees. Similar conditions of the vast bare lands can be observed in Al-Wozyah, which also showed high CO_2 concentrations. Unlike Al-Hofuf, the Al-Oyon site covered large areas of urban and bare lands, but the concentration of CO_2 in it was low. This is due to the less transportation movement in Al-Oyon, as it is considered a suburban area. Also, palm orchards and farms located in the southeast of Al-Oyon may contribute to reducing CO_2 emissions. Urbanisation in arid and semiarid regions can significantly impact CO_2 concentrations and emissions estimated for different LULC types [69,70]. The relatively low CO_2 concentration in Al-Battaliyah and Al-Taraf might be due to the extensive vegetation covers extended in these sites. Urban vegetation can play a vital role in exchanging CO_2 concentrations in cities due to plant photosynthesis [40]. Also, urban vegetation is a beneficial planning strategy to control the heat island and improve the energy efficiency of buildings in urban cities [71].

The spatial distribution of CO_2 concentration in the study sites shows that its levels vary according to the areas occupied by the different LULC types (Figure 9). In Al-Oyon, the low values of CO_2 concentration ranging from 377 to 382 ppm occurred in cropland and date palm land-use systems, while the high 386–392 ppm was associated with the bare and urban lands (Figure 9a). Most of

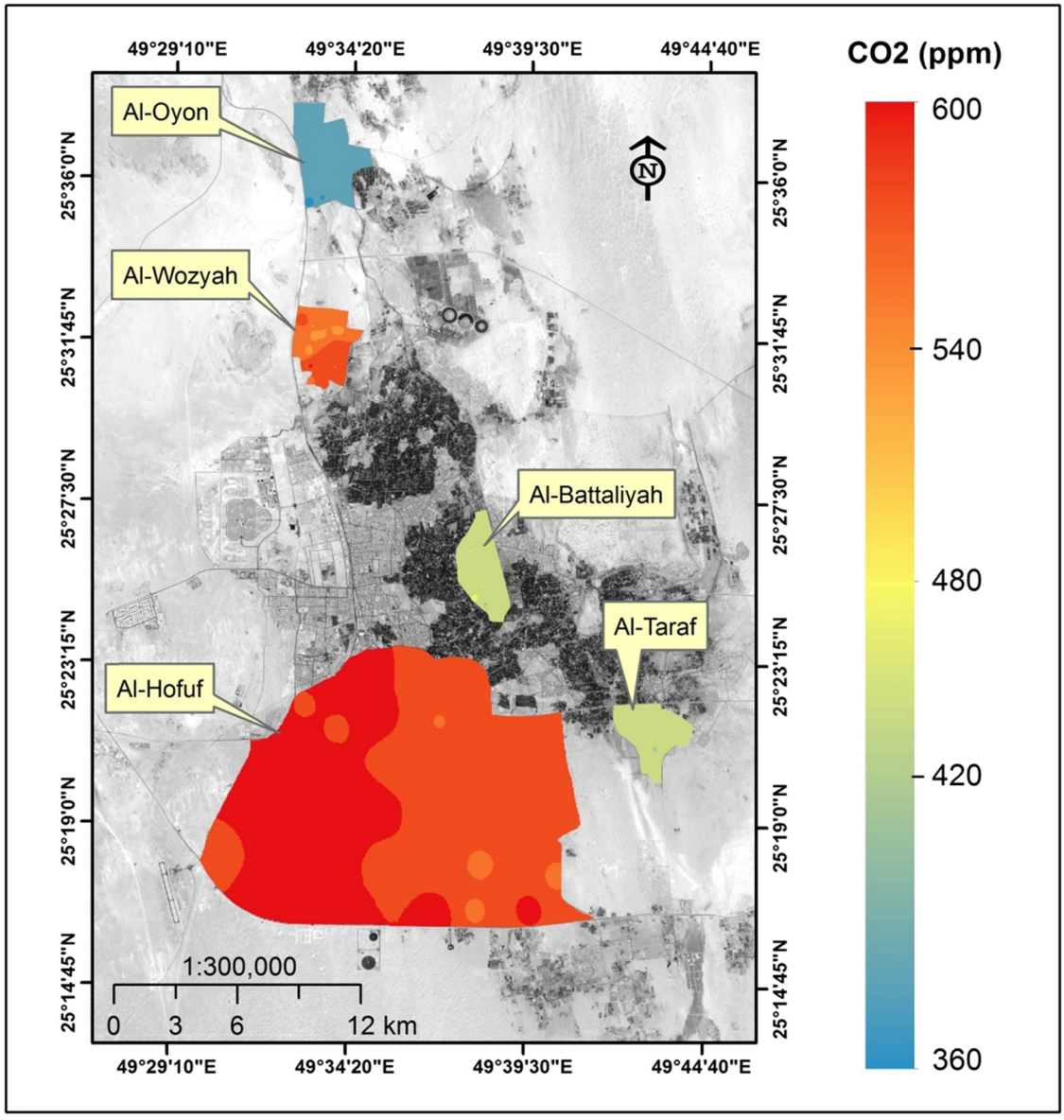

Figure 6: The spatial distribution of CO_2 levels over the study sites.

the area in Al-Wozyah is covered by bare lands, which shows CO_2 levels of 559–561 ppm compared to 570 ppm detected over the small area occupied by the urban land (Figure 9b). The high CO_2 levels resulting from the bare and urban lands in Al-Wozyah have affected the amount of CO_2 concentration that appeared over the date palm and cropland areas showing CO_2 levels around 546 ppm. In Al-Battaliyah, the date palm was the dominant LULC system showing CO_2 concentration levels of 446–452 ppm, followed by the cropland with 440–446 ppm, bare land with 453–458 ppm, and finally urban land with 458–464 ppm (Figure 9c). The domination of bare lands in Al-Hofuf resulted in CO_2 levels of 560–576 ppm, while the vast areas occupied by the urban lands raised the CO_2 levels to 580–594 ppm (Figure 9d). The CO_2 concentration levels in Al-Taraf ranged from 441 to 445 ppm for the date palm and cropland systems, while it ranged between 447 and 449 ppm for the bare land and almost around 450 ppm for the urban land (Figure 9e).

The CO_2 concentration mean values detected for the different LULC types in the study area showed it was 560, 535, 515, and 484 ppm for the urban land, bare land, cropland, and date palm, respectively. Thus, the increasing and decreasing of the CO_2 levels across the different LULC types over the study sites (Figure 10) are mainly attributed to the movement of active winds during the summer,

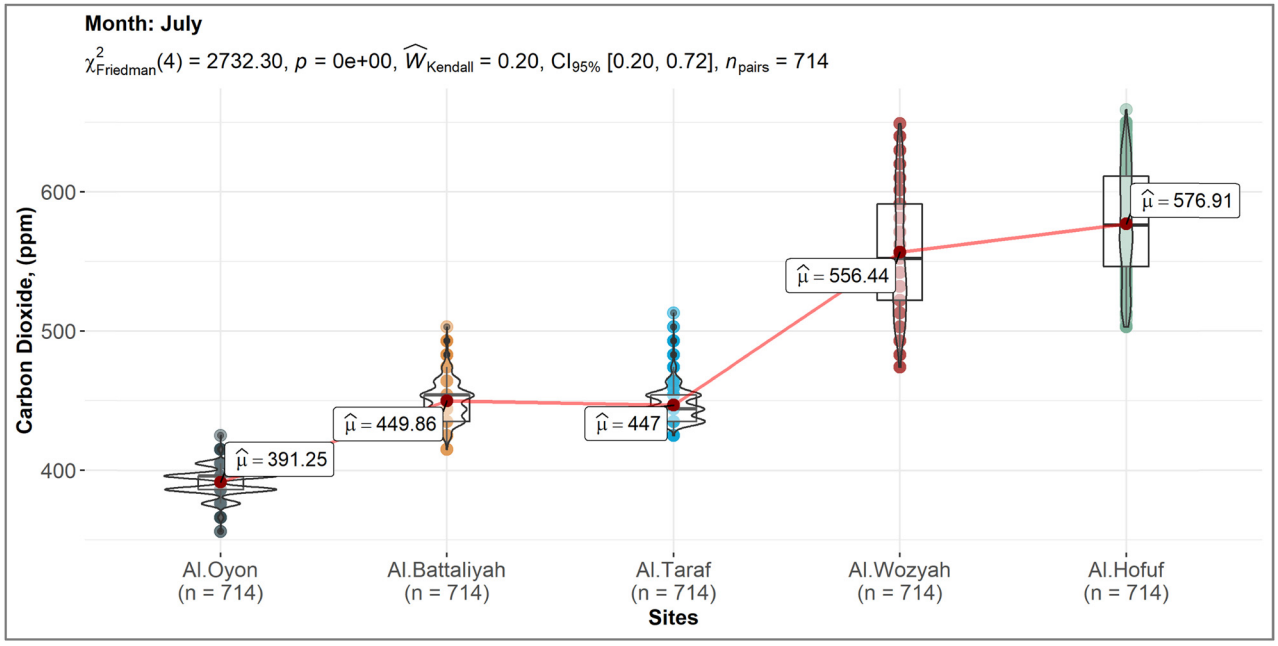

Figure 7: Comparison of the CO_2 level mean values in the different study sites.

Table 6: Pairwise comparison of CO_2 levels between the different study sites

Friedman coefficient (X^2) = 2,732		
Degree of freedom (df) = 4		
Probability (P) < 0.001		
Sites pair	**Statistic**	***P***
Al-Oyon–Al-Battaliyah	90.14*	<0.001
Al-Oyon–Al-Taraf	83.22*	<0.001
Al-Oyon–Al-Wozyah	174.73*	<0.001
Al-Oyon–Al-Hofuf	229.36*	<0.001
Al-Battaliyah–Al-Taraf	6.91ns	<0.001
Al-Battaliyah–Al-Wozyah	84.60*	<0.001
Al-Battaliyah–Al-Hofuf	139.23*	<0.001
Al-Taraf–Al-Wozyah	91.51*	<0.001
Al-Taraf–Al-Hofuf	146.14*	<0.001
Al-Wozyah–Al-Hofuf	54.63*	<0.001

* = Significant; ns = not significant.

where its speed ranged between 5 and 8 km/h in the north and north-west direction of the study area [72]. Moreover, the urban atmospheric CO_2 concentrations variation is expected in the Middle East region. For instance, in the Gaza City of Palestine, this variation ranged between 300 and 900 ppm showing higher levels during working days than at the weekend [73]. Therefore, vegetated areas can act as mitigation measure that reduce CO_2 emissions and lower the air temperature depending on the wind speed and direction from one site to another. Nevertheless, Pataki et al. [74] have indicated the limited role of urban trees in reducing GHG emissions and pollution over vast areas and environmental conditions. However, urban trees are more useful for climate and pollution adaptation approaches than emission reduction. This is because of the limitation in spaces that constrain tree canopies compared to the amount of emissions.

Agriculture and land-use change contribute to about 21% of the global GHG emission. Therefore, to achieve low CO_2 levels, several measures can be applied. These include re-prioritising land-use systems in urban and rural areas, controlled irrigation, crop diversification, and cover crops [75]. However, land use draws attention to be used as a policy tool for carbon reduction and low-carbon planning [76]. This is because it has changed the Earth's carbon cycle by influencing the natural carbon sources and sinks like cropland, grassland, and forests [77,78].

Vegetation has crucial environmental functions in urban areas since it removes pollutants [79]. Also, vegetation cover helps in reducing energy consumption in urban areas and hence improves their climate [80]. Therefore, appearing vegetation cover in the urban environment is essential for heat island mitigation in cities [81]. However, CO_2 was the major driving factor for vegetation cover changes [82]. Moreover, the study area faces a lack of precipitation, which might be one of the main causes of CO_2 concentration increase [83]. The relationship between

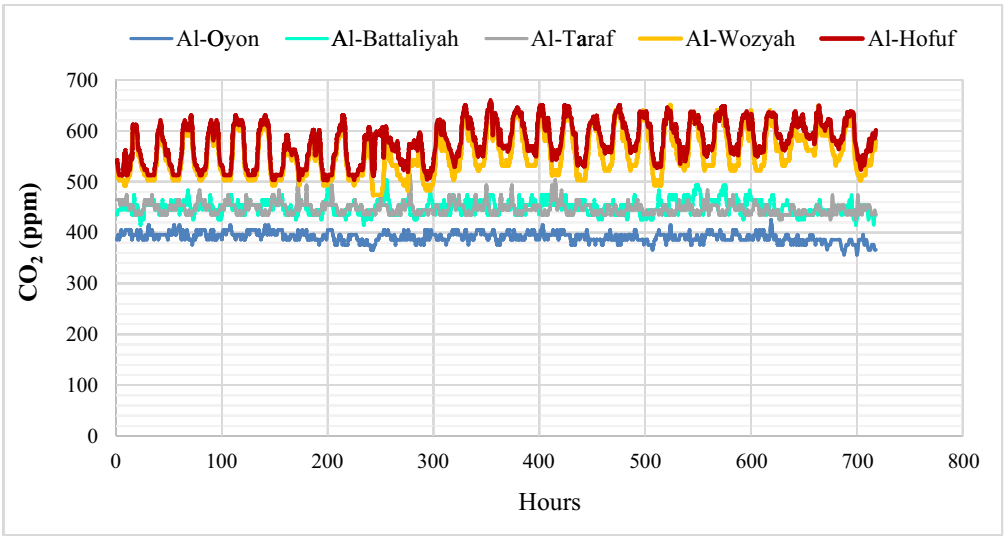

Figure 8: Hourly time series for the CO_2 concentration in the different study sites.

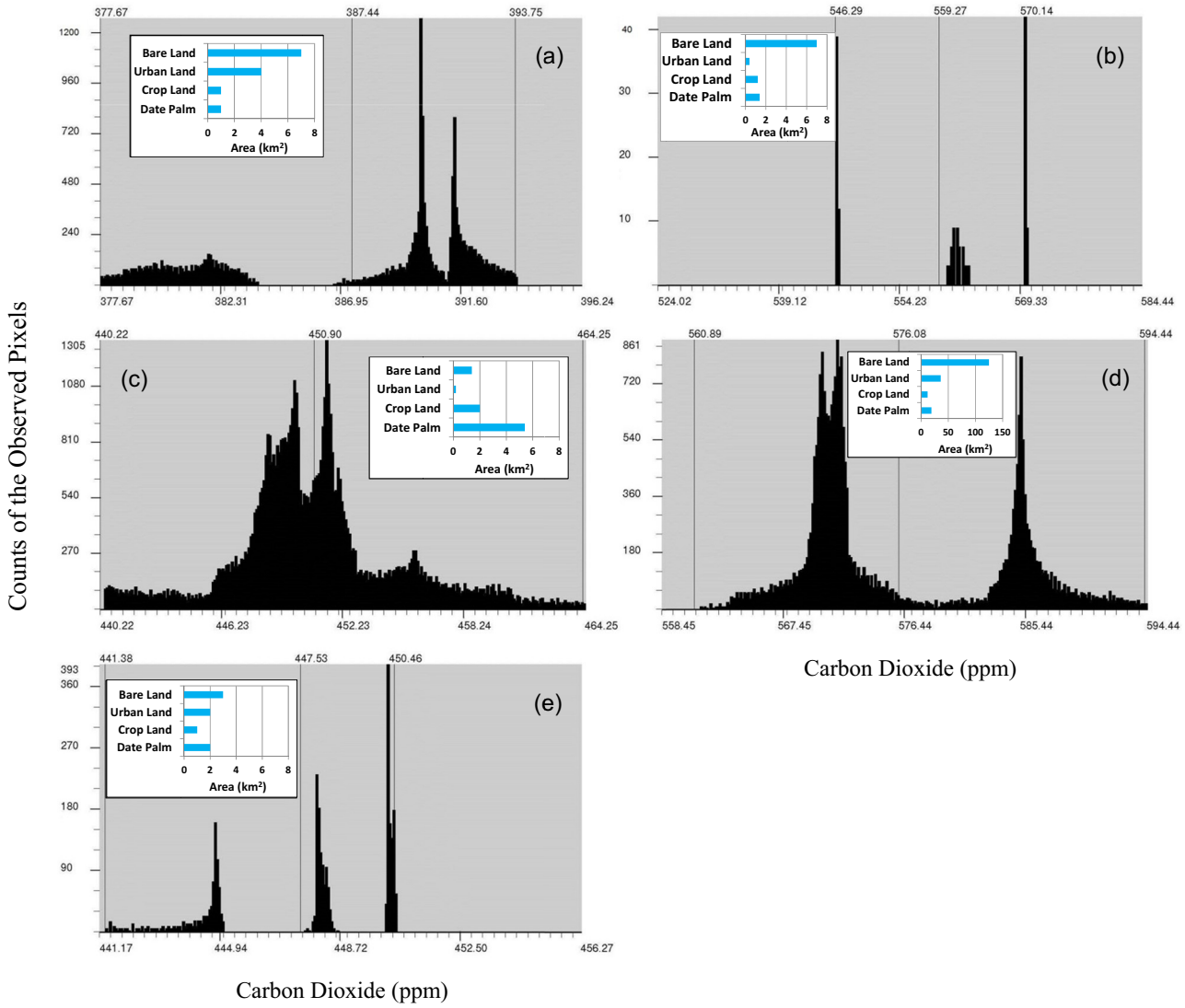

Figure 9: The spatial distribution of CO_2 concentration over the different LULC types. (a) Al-Oyon, (b) Al-Wozyah, (c) Al-Battaliyah, (d) Al-Hofuf and (e) Al-Taraf.

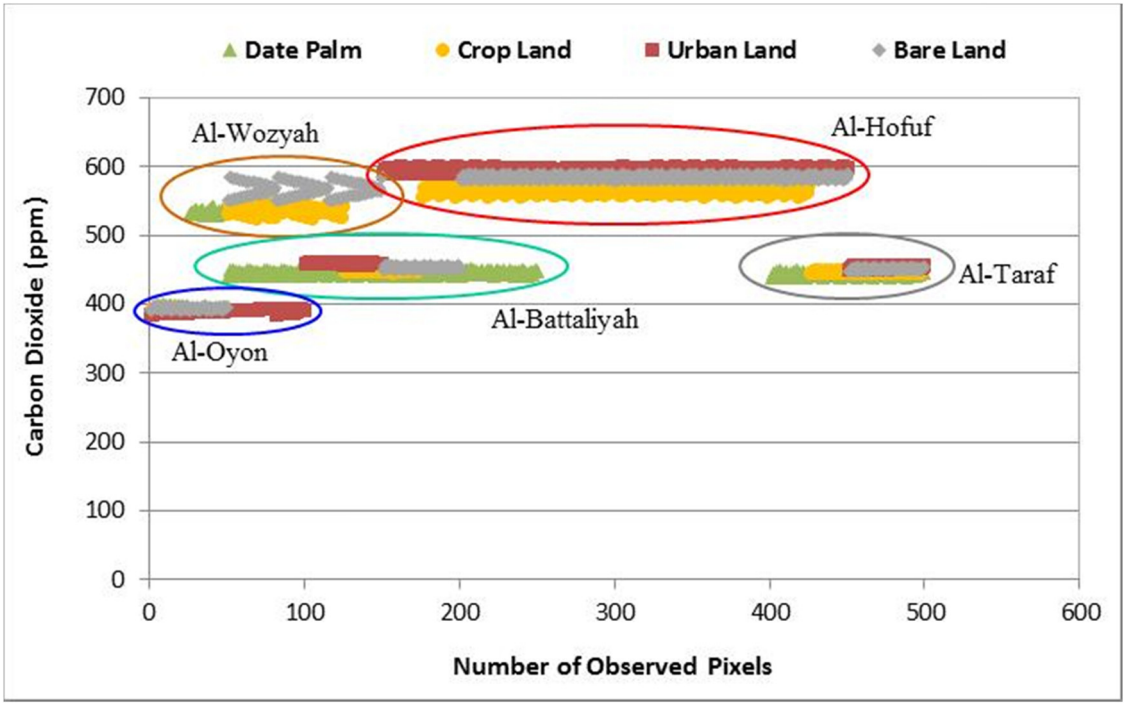

Figure 10: The patterns of CO_2 for the different LULC types within the study sites.

urban form and CO_2 emissions indicated that less complex cities have lower CO_2 emissions, but dense cities have greater per capita CO_2 emissions [84]. Also, socioeconomic factors of industrial structure, population density, and economic development level were the main drivers of CO_2 emissions in urban form areas [85].

4 Conclusions

The world faces a continuous increase in atmospheric CO_2 concentrations due to climate change and the consequences of land-use change. Therefore, continuous monitoring of CO_2 concentrations in the air at regional and local scales will help drive global efforts to reduce CO_2 emissions. In addition, site monitoring of CO_2 will provide the local policymakers with the needed information to formulate policies and strategies that cut down the levels of CO_2 in the atmosphere.

In this study, the CO_2 concentrations in the air were monitored for 1 month during the summertime in July. The tested sites covered different LULC types of urban and suburban areas. The hourly recorded data of the CO_2 showed significant variations between the study sites. For example, a maximum mean value of 577 ppm was detected in a site dominated by urban lands. However, the hourly recorded CO_2 concentrations showed a maximum value of 659 ppm during the peak time of human transportation and movement. Nevertheless, the patterns of the CO_2 levels showed significant variations across the different LULC types over the study sites.

The sensors and methodology used in this study provided valuable information about the CO_2 concentrations and levels over a specific site. However, there is a real challenge in designing a sensor network capable of continuously detecting CO_2 in large open space areas over a long time. In addition, modelling CO_2 variation over time due to the LULC changes might help predict the best practices for land-use management that can reduce the CO_2 levels in the atmosphere. Therefore, adequate management of agricultural lands and reducing CO_2 emissions and pollution from crop and animal production will help preserve and enhance the air quality for most LULC types dominated in the study area.

Acknowledgments: The authors would like to thank the anonymous reviewers for their contribution to the improvement of the manuscript. Also, we would like to express our gratitude to Dr. Yousef Ahmed Alkhamis, the director of the Water Studies Center at King Faisal University, for his continuous support.

Funding information: This work was supported by the Deanship of Scientific Research, King Faisal University, Saudi Arabia (grant number NA000251).

Author contributions: A.O.A. set the concept and the methodology; A.O.A., K.B.T., and F.I.Z. carried out field data collection; K.B.T. performed software and formal analysis of the data, and writing the original draft of the manuscript; F.I.Z. did the review writing and editing of the manuscript and the work supervision. All authors have read and agreed to the published version of the manuscript.

Conflict of interest: Authors state no conflict of interest.

Data availability statement: The datasets generated during and/or analyzed during the current study are available from the corresponding author on reasonable request.

References

[1] Kuncoro CBD, Luo WJ, Selamet MR, Sri MN, Kurniawan AS, Kuan YD. Automatic wireless ambient air and weather condition monitoring system for outdoor environment monitoring applications. Sens Mater. 2020;32(1):337–56.
[2] Qiu L, Liu X, Hao Y. Quantitative assessment of the role of doubled CO_2 and associated climate change in the vegetation dynamics and hydrological cycle in the Sino-Mongolia arid and semi-arid region. Stoch Environ Res Risk Assess. 2017;31:785–97.
[3] Gao Y, Li X, Liu L, Jia R, Yang H, Li G, et al. Seasonal variation of carbon exchange from a revegetation area in a Chinese desert. Agric Meteorol. 2012;156:134–42.
[4] Wang H, Li X, Xiao J, Ma M, Tan J, Wang X, et al. Carbon fluxes across alpine, oasis, and desert ecosystems in northwestern China: the importance of water availability. Sci Total Environ. 2019;697:133978.
[5] Wang Y, Nakayama M, Watanabe K, Yagi M, Nishikawa M, Fukunaga M. The NDIR CO_2 monitor with smart interface for global networking. IEEE Trans Instrum Meas. 2005;54:1634–9.
[6] United Nation. World's population increasingly urban with more than half living in urban areas. 2014 [cited 2014 July 10]. https://www.un.org/en/development/desa/news/population/world-urbanization-prospects-2014.html.
[7] Asakawa T, Kanno N, Tonokura K. Diode laser detection of greenhouse gases in the near-infrared region by wavelength modulation spectroscopy: pressure dependence of the detection sensitivity. Sensors. 2010;10:4686–99.
[8] Bezyk Y, Oshurok D, Dorodnikov M, Sówka I. Evaluation of the CALPUFF model performance for the estimation of the urban ecosystem CO_2 flux. Atmos Pollut Res. 2021;12:213–30.
[9] Lawrence PJ, Chase TN. Investigating the climate impacts of global land cover change in the community climate system model. Int J Climatol. 2010;30:2066–87.
[10] Ciais P, Gasser T, Paris J, Caldeira K, Raupach MR, Canadell J, et al. Attributing the increase in atmospheric CO_2 to emitters and absorbers. Nat Clim Chang. 2013;3:926–30.
[11] Mahowald NM, Randerson JT, Lindsay K, Munoz E, Doney SC, Lawrence P, et al. Interactions between land use change and carbon cycle feedbacks. Glob Biogeochem Cycles. 2017;31:96–113.
[12] Hua W, Chen H, Suna S, Zhou L. Assessing climatic impacts of future land use and land cover change projected with the CanESM2 model. Int J Climatol. 2015;35:3661–7.
[13] Tubiello F, Salvatore M, Ferrara AF, House J, Federici S, Rossi S, et al. The contribution of agriculture, forestry and other land use activities to global warming, 1990–2012. Glob Change Biol. 2015;21:2655–60.
[14] Szogs S, Arneth A, Anthoni P, Doelman JC, Humpenöder F, Popp A, et al. Impact of LULCC on the emission of BVOCs during the 21st century. Atmos Environ. 2017;165:73–87.
[15] Houghton RA. Balancing the global carbon budget. Annu Rev Earth Planet Sci. 2007;35:313–47.
[16] Liu Y, Wu C, Wang X, Jassal RS, Gonsamo A. Impacts of global change on peak vegetation growth and its timing in terrestrial ecosystems of the continental US. Glob Planet Change. 2021;207:103657.
[17] Zhao ZQ, He BJ, Li LG, Wang HB, Darko A. Profile and concentric zonal analysis of relationships between land use/land cover and land surface temperature: case study of Shenyang, China. Energy Build. 2017;155:282–95.
[18] Zhao Z, Sharifi A, Dong X, Shen L, He BJ. Spatial variability and temporal heterogeneity of surface urban heat island patterns and the suitability of local climate zones for land surface temperature characterization. Remote Sens. 2021;13:4338.
[19] Yasuda T, Yonemura S, Tani A. Comparison of the characteristics of small commercial NDIR CO_2 sensor models and development of a portable CO_2 measurement device. Sensors. 2012;12:3641–55.
[20] Ramamurthy P, Pardyjak ER. Toward understanding the behavior of carbon dioxide and surface energy fluxes in the urbanized semi-arid Salt Lake Valley, Utah, USA. Atmos Environ. 2011;45:73–84.
[21] Pataki DE, Alig RJ, Fung AS, Golubiewski NE, Kennedy CA, Mcpherson EG, et al. Urban ecosystems and the North American carbon cycle. Glob Change Biol. 2006;12:2092–2102.
[22] Feng H, Zou B. Satellite-based separation of climatic and surface influences on global aerosol change. Int J Remote Sens. 2020;41(14):5443–56.
[23] Crawford B, Grimmond CSB, Christen A. Five years of carbon dioxide fluxes measurements in a highly vegetated suburban area. Atmos Environ. 2011;45(4):896–905.
[24] Pérez-Ruiz ER, Vivoni ER, Templeton NP. Urban land cover type determines the sensitivity of carbon dioxide fluxes to precipitation in Phoenix, Arizona. PLoS ONE. 2020;15(2):e0228537.
[25] Ng BJL, Hutyra LR, Nguyen H, Cobb AR, Kai FM, Harvey C, et al. Carbon fluxes from an urban tropical grassland. Environ Pollut. 2015;203:227–34.
[26] Liu C, Liang Y, Zhao Y, Liu S, Huang C. Simulation and analysis of the effects of land use and climate change on carbon dynamics in the Wuhan city circle area. Int J Environ Res Public Health. 2021;18:11617.

[27] Lee E, Zeng FW, Koster RD, Ott LE, Mahanama S, Weir B, et al. Impact of a regional U.S. drought on land and atmospheric carbon. J Geophys Res Biogeosci. 2020;125:e2019JG005599.
[28] Wu S, Mickley LJ, Kaplan JO, Jacob DJ. Impacts of changes in land use and land cover on atmospheric chemistry and air quality over the 21st century. Atmos Chem Phys. 2012;12:1597–609.
[29] Ward DS, Mahowald NM, Kloster S. Potential climate forcing of land use and land cover change. Atmos Chem Phys. 2014;14:12701–24.
[30] Hua W, Haishan H, Sun S, Zhou L. Assessing climatic impacts of future land use and land cover change projected with the CanESM2 model. Int J Climatol. 2015;35:3661–75.
[31] Xi Y, Peng S, Ciais P, Guimberteau M, Li Y, Piao S, et al. Contributions of climate change, CO_2, land-use change, and human activities to changes in river flow across 10 Chinese Basins. J Hydrometeorol. 2018;9:1900–914.
[32] Chadwick R, Ackerley D, Ogura T, Dommenget D. Separating the influences of land warming, the direct CO_2 effect, the plant physiological effect, and SST warming on regional precipitation changes. J Geophys Res Atmos. 2019;124:624–40.
[33] Friedlingstein P, O'Sullivan M, Jones MW, Andrew RM, Hauck J, Olsen A, et al. Global Carbon Budget 2020. Earth Syst Sci Data. 2020;12:3269–340.
[34] Bhide A, Jagannath B, Tanak A, Willis R, Prasad S. CLIP. Carbon dioxide testing suitable for low power microelectronics and IOT interfaces using room temperature ionic liquid platform. Sci Rep. 2020;10:2557.
[35] Fine GF, Cavanagh LM, Afonja A, Binions R. Metal oxide semiconductor gas sensors in environmental monitoring. Sensors. 2010;10:5469–502.
[36] Jiao Z, Chen F, Su R, Huang X, Liu W, Liu J. Study on the characteristics of Ag doped CuO–$BaTiO_3$ CO_2 sensors. Sensors. 2002;2:366–73.
[37] Mandayo GG, Herrán J, Castro-Hurtado I, Castaño E. Performance of a CO_2 impedimetric sensor prototype for air quality monitoring. Sensors. 2011;11:5047–57.
[38] Hannon A, Li J. Solid state electronic sensors for detection of carbon dioxide. Sensors. 2019;19:3848.
[39] Chu CS, Lo YL. Fiber-optic carbon dioxide sensor based on fluorinated xerogels doped with HPTS. Sens Actuators B Chem. 2008;129:120–5.
[40] Martin CR, Zeng N, Karion A, Dickerson RR, Ren X, Turpie BN, et al. Evaluation and environmental correction of ambient CO_2 measurements from a low-cost NDIR sensor. Atmos Meas Tech. 2017;10:2383–95.
[41] Brown SL, Goulsbra CS, Evans MG, Heat T, Shuttleworth E. Low cost CO_2 sensing: a simple microcontroller approach with calibration and field use. HardwareX. 2020;8:e00136.
[42] Shusterman AA, Teige VE, Turner AJ, Newman C, Kim J, Cohen RC. The Berkeley atmospheric CO_2 observation network: initial evaluation. Atmos Chem Phys. 2016;16:13449–63.
[43] Li W, Ciais P, Peng S, Yue C, Wang Y, Thurner M, et al. Land-use and land-cover change carbon emissions between 1901 and 2012 constrained by biomass observations. Biogeosciences. 2017;14:5053–67.
[44] Wang G, Han Q, de vries B. The multi-objective spatial optimization of urban land use based on low-carbon city planning. Ecol Indic. 2021;125:107540.
[45] Al-Taher AA. Estimation of potential evapotranspiration in Al-Hassa oasis, Saudi Arabia. GeoJournal. 1992;26(3):371–9.
[46] Turk KGB, Aljughaiman AS. Land use/land cover assessment as related to soil and irrigation water salinity over an oasis in arid environment. Open Geosci. 2020;2:220–31.
[47] Ellis EA, Baerenklau KA, Marcos-Martínez R, Chávez E. Land use/land cover change dynamics and drivers in a low-grade marginal coffee growing region of Veracruz, Mexico. Agrofor Syst. 2010;80:61–84.
[48] Rahman MT, Aldosary AS, Mortoja MDG. Modeling future land cover changes and their effects on the land surface temperatures in the Saudi Arabian eastern coastal city of Dammam. Land. 2017;6:36.
[49] Abdallah S, Abdelmohemen M, Hemdan S, Ibrahem K. Assessment of land use/land cover changes induced by Jizan Dam, Saudi Arabia, and their effect on soil organic carbon. Arab J Geosci. 2019;12:350.
[50] Mundia CN, Aniya M. Dynamics of land use/cover changes and degradation of Nairobi city, Kenya. Land Degrad Dev. 2006;17:97–108.
[51] Congalton RG, Green K. Assessing the accuracy of remotely sensed data, principles and practices. 3rd edn. Boca Raton, London, New York: CRC Press, Taylor & Francis Group; 2019.
[52] Telaire 7001 Manufacturers Manual. 2014 [cited 2014 Oct]. https://www.onsetcomp.com/support/tech-note/telaire-7001-manufacturers-manual/.
[53] Sheldon MR, Fillyaw MJ, Thompson WD. The use and interpretation of the Friedman test in the analysis of ordinal-scale data in repeated measures designs. Physiother Res Int. 1996;1(4):221–8.
[54] Pereira DG, Afonso A, Medeiros FM. Overview of Friedman's test and post-hoc analysis. Commun Stat Simul Comput. 2015;44(10):2636–53.
[55] Friedman M. A comparison of alternative tests of significance for the problem of m rankings. Ann Math Stat. 1940;11:86–92.
[56] Statistics Solutions. Friedman Test, Kendall's W, Cochran's Q: Significance Tests for More Than Two Dependent Samples. 2013 [cited 2013 Dec 21]. https://www.statisticssolutions.com/free-resources/directory-of-statistical analyses/significance-tests-for-more-than-two-dependent-samples-friedman-test-kendalls-w-cochrans-q/.
[57] Zaiontz C Real Statistics Using Excel; 2020 [cited 2020 June 15]. www.real-statistics.com.
[58] ArcGIS Help Library. 2013 [cited 2013 Sep 18]. http://desktop.arcgis.com/en/arcmap/latest/get-started/main/get-started-witharcmap.htm.
[59] Hill T, Lewicki P. Statistics methods and applications. Tulsa, OK: StatSoft; 2007.
[60] Baskauf SJ. Introduction to Biological Sciences Lab (BSCI 1510L) Excel Reference and Statistics Manual. Nashville, TN: Vanderbilt University; 2016 [cited 2016 April 12; updated 2020 Aug 24]. http://researchguides.library.vanderbilt.edu/bsci1510L.
[61] Madugundu R, Al-Gaadi KA, Patil VC, Tola E. Detection of land use and land cover changes in dirab region of Saudi Arabia using remotely sensed imageries. Am J Environ Sci. 2014;10:8–18.
[62] Al-Ahmadi F, Hames A. Comparison of four classification methods to extract land use and land cover from raw satellite

images for some remote arid areas, kingdom of Saudi Arabia. J King Saud Univ Sci. 2009;20:167–9.
[63] Pigliautile I, Marseglia G, Pisello AL. Investigation of CO_2 variation and mapping through wearable sensing techniques for measuring pedestrians' exposure in urban areas. Sustainability. 2020;12:3936.
[64] Buchholz RR, Paton-Walsh C, Griffith DWT, Kubistin D, Caldow C, Fisher JA, et al. Source and meteorological influences on air quality (CO, CH_4 & CO_2) at a Southern Hemisphere urban site. Atmos Environ. 2016;126:274–89.
[65] UN-Habitat. Saudi Arabia. 2022 [cited 2022 May 11]. https://unhabitat.org/saudi-arabia.
[66] Bergeron O, Strachan IB. CO_2 sources and sinks in urban and suburban areas of a northern mid-latitude city. Atmos Environ. 2011;45(8):564–1573.
[67] Wilkinson MJ, Monson RK, Trahan N, Lee S, Brown E, Jackson RB, et al. Leaf isoprene emission rate as a function of atmospheric CO_2 concentration. Glob Change Biol. 2009;15:1189–200.
[68] Possell M, Hewitt CN. Isoprene emissions from plants are mediated by atmospheric CO_2 concentrations. Glob Change Biol. 2011;17:1595–610.
[69] Koerner B, Klopatek J. Carbon fluxes and nitrogen availability along an urban–rural gradient in a desert landscape. Urban Ecosyst. 2010;13(1):1–21.
[70] Song J, Wang ZH, Wang C. Biospheric and anthropogenic contributors to atmospheric CO_2 variability in a residential neighborhood of Phoenix, Arizona. J Geophys Res Atmos. 2017;22(6):3317–29.
[71] Wang Y, Akbari H. The effects of street tree planting on urban heat island mitigation in Montreal. Sustain Cities Soc. 2016;122–8.
[72] Alghannam AO, Al-Qahtnai MRA. Impact of vegetation cover on urban and rural areas of arid climates. Aust J Agric Eng. 2012;3(1):1–5.
[73] Salem MZ, Almuzaini RF, Kishawi YS. The impact of road transport on CO_2 atmospheric concentrations in Gaza city (Palestine), and urban vegetation as a mitigation measure. Pol J Environ Stud. 2017;26(5):2175–88.
[74] Pataki DE, Alberti M, Cadenasso ML, Felson AJ, McDonnell MJ, Pincetl S, et al. Benefits and limits of urban tree planting for environmental and human health. Front Ecol Evol. 2021;9:603757.
[75] Barnes D, Corwin S, Kaszynski K, Pankratz DM, McGuinty E Policy considerations for a low-carbon food and land-use system. Deloitte Global, 2021 [cited 2021 Nov 23]. https://www2.deloitte.com/global/en/pages/about-deloitte/articles/policy-considerations-for-low-carbon-food-and-land-use-system.html.
[76] Zhang R, Matsushima K, Kobayashi K. Can land use planning help mitigate transport-related carbon emissions? A case of Changzhou. Land Use Policy. 2018;74:32–40.
[77] Houghton RA, Hacker JL, Lawrence KT. The U.S. carbon budget: contributions from land-use change. Science. 1999;285:574–8.
[78] Caspersen JP, Pacala SW, Jenkins JC, Hurtt GC, Moorcroft PR, Birdsey RA. Contributions of land-use history to carbon accumulation in U.S. Science. 2000;290:1148–51.
[79] Leung DY, Tsui JK, Chen F, Yip WK, Vrijmoed LL, Liu CH. Effects of urban vegetation on urban air quality. Landsc Res. 2011;36:173–88.
[80] Liu Z, Brown RD, Zheng S, Jiang Y, Zhao L. Ani-depth analysis of the effect of trees on human energy fluxes. Urban Urban Green. 2020;50:126646.
[81] Ferrini F, Fini A, Mori J, Gori A. Role of vegetation as a mitigating factor in the urban context. Sustainability. 2020;12:4247.
[82] Mu B, Zhao X, Wu D, Wang X, Zhao J, Wang H, et al. Vegetation cover change and its attribution in China from 2001 to 2018. Remote Sens. 2021;13:496.
[83] Yin S, Wang X, Tani H, Zhang X, Zhong G, Sun Z, et al. Analyzing temporo-spatial changes and the distribution of the CO_2 concentration in Australia from 2009 to 2016 by greenhouse gas monitoring satellites. Atmos Environ. 2018;192:1–12.
[84] Makido Y, Dhakal S, Yamagata Y. Relationship between urban form and CO_2 emissions: evidence from fifty Japanese cities. Urban Clim. 2012;2:55–67.
[85] Guo R, Leng H, Yuan Q, Song S. Impact of urban form on CO_2 emissions under different socioeconomic factors: evidence from 132 small and medium-sized cities in China. Land. 2022;11:713.